Available online at www.sciencedirect.com
SCIENCE DIRECT®
C. R. Geoscience 335 (2003) 691–699
COMPTES RENDUS GEOSCIENCE

Tectonics

New structural and petrologic data on Mesozoic schists in the Rhodope (Bulgaria): geodynamic implications

Nikolay G. Bonev *, Gérard M. Stampfli

Institute of Geology and Paleontology, University of Lausanne, BFSH 2, CH-1015 Lausanne, Switzerland

Received 25 February 2003; accepted 23 June 2003

Presented by Jacques Angelier

Abstract

Structural analysis of low-grade rocks highlights the allochthonous character of Mesozoic schists in southeastern Rhodope, Bulgaria. The deformation can be related to the Late Jurassic–Early Cretaceous thrusting and Tertiary detachment faulting. Petrologic and geochemical data show a volcanic arc origin of the greenschists and basaltic rocks. These results are interpreted as representing an island arc-accretionary complex related to the southward subduction of the Meliata–Maliac Ocean under the supra-subduction back-arc Vardar ocean/island arc system. This arc-trench system collided with the Rhodope in Late Jurassic times. ***To cite this article: N.G. Bonev, G.M. Stampfli, C. R. Geoscience 335 (2003).***

Résumé

Nouvelles données structurales et pétrologiques sur les schistes mésozoïques dans le Rhodope (Bulgarie) : implications géodynamiques. L'analyse structurale de roches de faible métamorphisme souligne le caractère allochtone des schistes mésozoïques du Sud-Est du Rhodope, en Bulgarie. La déformation peut être reliée au charriage du Jurassique supérieur–Crétacé inférieur et à la formation de failles de détachement au Tertiaire. Les données pétrologiques et géochimiques indiquent une origine de type arc volcanique pour les schistes verts et les roches basaltiques. Ces résultats sont interprétés comme représentant un complexe accrétionnaire d'arc insulaire en liaison avec la subduction vers le sud de l'océan Meliata–Maliac sous la supra-subduction d'arrière-arc du système océan Vardar/arc insulaire. Ce système d'accrétion est entré en collision avec le Rhodope au Jurassique supérieur. ***Pour citer cet article : N.G. Bonev, G.M. Stampfli, C. R. Geoscience 335 (2003).***

Keywords: Mesozoic schists; basalt extrusives; thin-skinned tectonics; Rhodope; Vardar Ocean; Bulgaria

Mots-clés : schistes mésozoïques ; extrusions basaltiques ; tectonique d'amincissement de croûte ; Rhodope ; océan Vardar ; Bulgarie

1. Introduction

Low-grade Mesozoic rocks in the southeastern Rhodope represent the uppermost tectono-stratigraphic unit of the Rhodope metamorphic pile. These weakly metamorphosed units, together with similar

* Corresponding author.
E-mail addresses: nikolay.bonev@igp.unil.ch (N.G. Bonev), Gerard.stampfli@igp.unil.ch (G.M. Stampfli).

1631-0713/$ – see front matter
doi:10.1016/S1631-0713(03)00122-6

units that extend from Samothraki Island to Chalkidiki Peninsula, were designated as the Circum-Rhodope Belt (CRB) [15] (Fig. 1A), found around the Rhodope complex. It separates the latter, through the Vardar suture, from the Pelagonian zone of the internal Hellenides. Studies in the Vardar zone have shown that ophiolites originated in a Mid-Late Jurassic back-arc basin of supra-subduction type [13], followed by an Early Cretaceous southwest-oriented ophiolite obduction [22]. Other studies have discarded the CRB concept [25]. However, the structural setting and geodynamic significance of Mesozoic schists in Bulgaria remain uncertain on the large-scale. The aim of this paper is to present new preliminary structural and petrologic data on these schists in the Bulgarian Rhodope. The results are interpreted in terms of lithologies generated in an intra-oceanic island arc. Geodynamic implications on the Late Jurassic–Early Cretaceous setting of the Vardar Ocean are discussed.

2. Geological setting

The Mesozoic schists crop out in scattered areas resting on the crystalline basement as remnants of a former nappe of wide regional extent. In previous studies, they have been subdivided into two units: Mandrica and Maglenica groups in Bulgaria [8], which can be correlated with the Makri and Drimos-Melia units in Greece [23], respectively. The whole sequence both in Bulgaria and Greece comprises greenschists at the base, overlain by a sequence of basic extrusives, referred to as Evros ophiolite [19], and anchi-metamorphic sediments at the top. Fossiliferous formations yielded Triassic (greenschists), and Jurassic to Late Cretaceous ages (anchi- to non-metamorphic) [5,7,20,31]. The apatite fission-track data of basic rocks define an interval comprised between 140–161 Ma in Thrace [4], and K–Ar hornblende analysis gave an age of 155 ± 7 Ma in Samothraki [33]. The allochthonous structure and inferred north-vergent thrusting is suggested through the general tectonic framework of the Balkanic orogen [8,14], or alternatively they are interpreted as southward-emplaced thrust sheet during the formation of Rhodope nappes [9]. Both crystalline basement and low-grade rocks are unconformably overlain by Upper Eocene to Miocene sediments [6] and intruded by Oligocene granitoids [10].

3. Tectono-stratigraphy and structural grain

Field observations based on different lithologies, metamorphic grade and strain pattern show that the whole sequence can be divided into several units (Fig. 1B). The basement sequence includes a lower orthogneiss unit composed mainly of two-mica gneisses, and an overlying upper marble-schist unit that consists of marbles intercalated with gneiss and schists. Both units correspond to the migmatite–orthogneiss sequence and upper terrane [9], or represent equivalents of the Kechros and Kimi Complexes [17], respectively. The basement lithologies show mineral assemblage $\mathrm{Qtz} + \mathrm{Pl} + \mathrm{Kfs} + \mathrm{Bt} + \mathrm{Ms} + \mathrm{Grt} + \mathrm{St}$ and amphibolite facies fabric. Slight retrogression of biotite altered to chlorite is observed at the contact between the two units, indicative of temperature decrease to less severe metamorphic conditions. The gneiss foliation and schistosity, defined by preferred orientation of minerals is flat lying, dipping to the NNE (Figs. 1B and 2), and bear mineral stretching lineation with consistent NNE–SSW trend. Associated shear sense criteria unequivocally indicates a top-to-the-SSW ductile shear (Fig. 3A). Strong mylonitic fabric in gneisses underlying the marble-schist unit has led to the interpretation of this contact as an important tectonic boundary. We interpret this ductile–brittle shear zone as a detachment fault that carries the Mesozoic schists in its hanging wall. As it parallels both the mylonitic fabric and marble horizons at the base of the marble-schist unit, and does not cut through the section, it more likely represents a decollement surface.

The Mesozoic sequence starts with a greenschist unit at the base, overlying the basement along the tectonic contact of presumably extensional origin. It is composed of actinolite–chlorite and garnet–mica schists, and phyllites. Mineral assemblages $\mathrm{Qtz} + \mathrm{Ms} + \mathrm{Act} + \mathrm{Chl} \pm \mathrm{Ep} \pm \mathrm{Grt}$ indicate greenschist facies metamorphism with temperatures below ca. 400°. The schistosity, associated to the metamorphic crystallizations, is affected by intense folding. Small-scale northeast-vergent tight folds that have axes oriented NW–SE appear as an earlier fold generation associated with syn-metamorphic actinolite

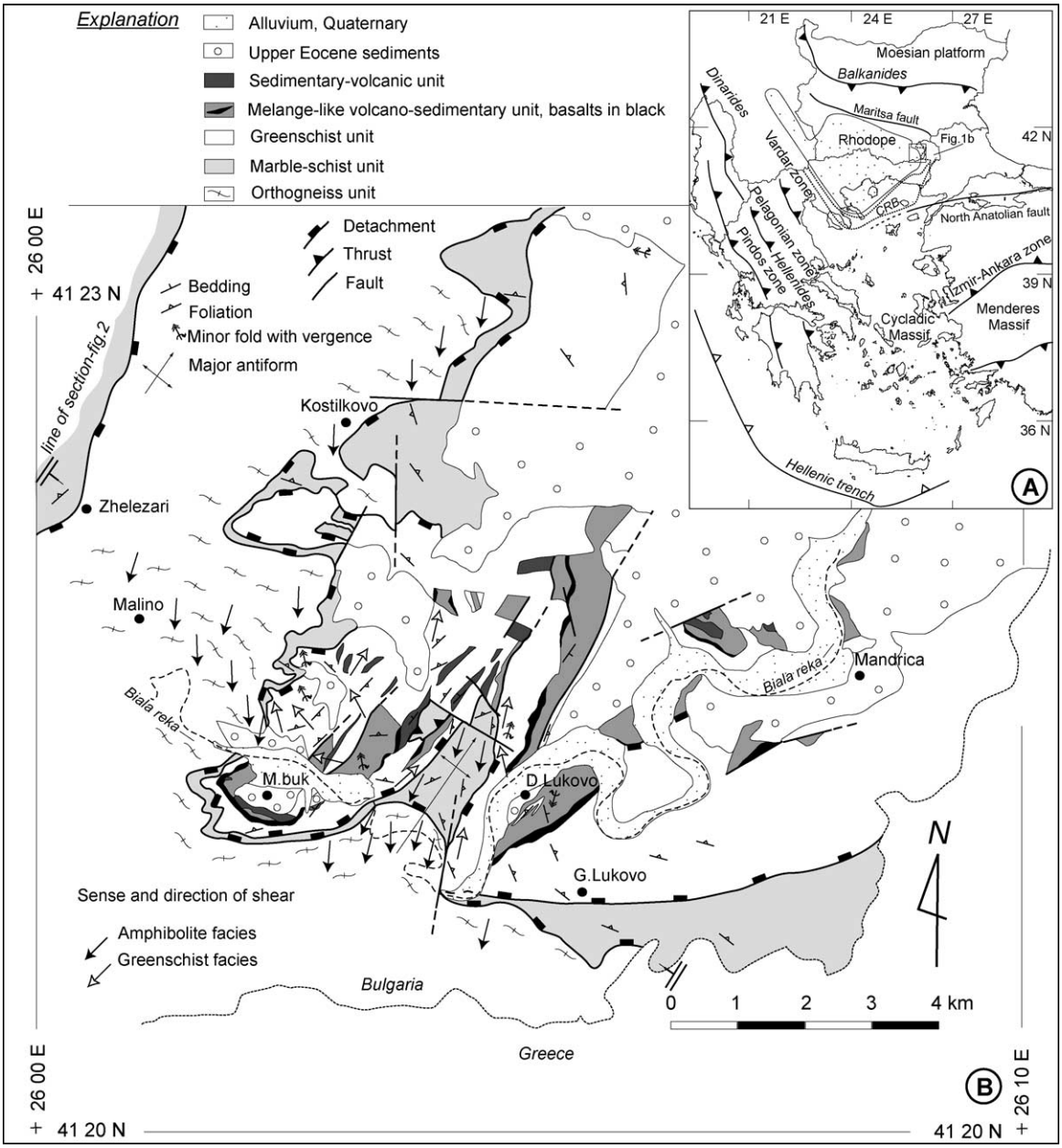

Fig. 1. (**A**) Extension of CRB in the north Aegean tectonic framework (stippled) and location of the studied area (framed). (**B**) Simplified map after [8] and personal data, and kinematic directions.

Fig. 1. (**A**) Extension de CRB dans le cadre tectonique nord-égéen (pointillés) et localisation de la région étudiée (encadré). (**B**) Carte simplifiée d'après [8] et données personnelles ; directions cinématiques.

laths. Asymmetric northwest-facing folds with discrete axial planar crenulation cleavage and NNE-SSW oriented axes are developed later, as deduced from crystallization–deformation relationships. Mineral elongation or stretching lineation is defined by aligned actinolite lath and streaky mica and chlorite flakes. It trends NW–SE, but swings to NE–SW at the vicinity of the tectonic contact that confines the

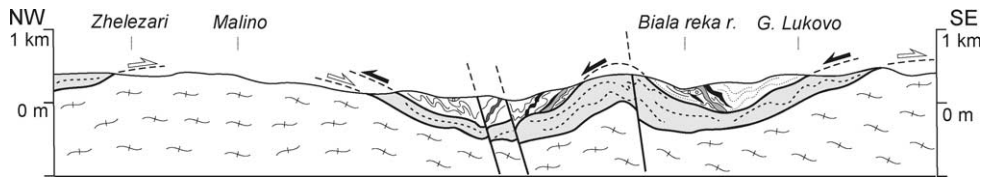

Fig. 2. Cross-section along the line shown in Fig. 1. Signatures as in Fig. 1; arrows: tectonic contacts.

Fig. 2. Coupe géologique localisée sur la Fig. 1. Mêmes signatures que sur la Fig. 1 ; flèches : contacts tectoniques.

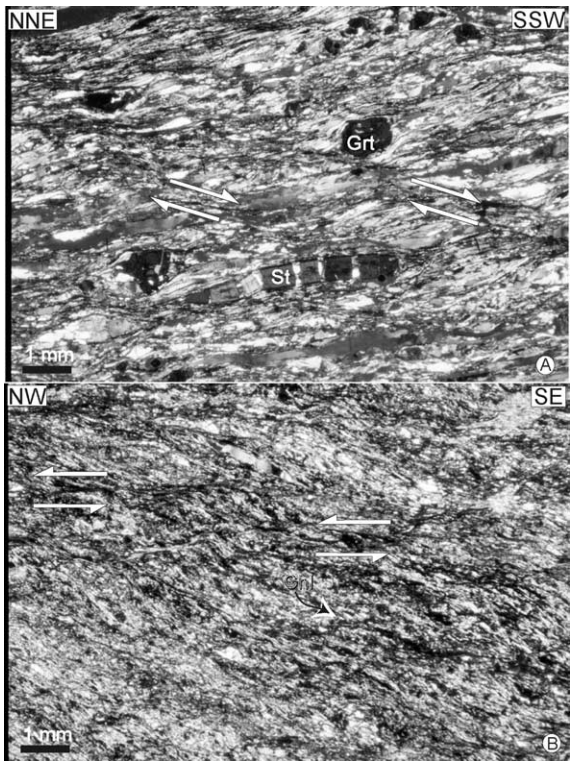

Fig. 3. (**A**) Microphotograph of mylonitic fabric in the detachment zone, Grt, garnet, St, staurolite, NX. (**B**) Microphotograph of shear fabric in quartz-chlorite schist, Chl, chlorite, NX.

Fig. 3. (**A**) Microphotographie de la fabrique des mylonites dans la zone de détachement, Grt, grenat, St, staurotide, NX. (**B**) Microphotographie de la fabrique cisaillante des schistes à quartz-chlorite, Chl, chlorite, NX.

greenschist unit from the marble-schist unit (Fig. 1B). Kinematic indicators demonstrate top-to-the-NW and NNE sense of shear (Fig. 3B) that occurred in greenschist facies. The reorientation of lineation at the vicinity of tectonically bounded kilometre-scale fold north of D. Lukovo is due to shortening that created this corrugated antiform of the basal detachment, whose axis parallels the kinematic direction.

The greenschist unit is overlain by tectonic or depositional contact of melange-like volcano-sedimentary unit. It consists of basalt lavas with Lower Jurassic radiolarian interlayers [31], Upper Permian siliciclastics [32] and Middle–Upper Triassic limestones [5] found as blocks in olistostromic packet, embedded in an Upper Jurassic–Lower Cretaceous shale-silty turbiditic matrix. The original sedimentary bedding of matrix lithologies is well preserved and only incipient seams-like cleavage is seen in thin sections, which suggests anchi-metamorphism.

The uppermost sedimentary-volcanogenic unit is composed of sandstones at the base, and andesito-basalt lavas and gabbro-diorites interbedded with marly and tufaceous sediments that yield Late Cretaceous foraminifera [7]. It overlies depositionally the greenschist and melange-like unit, and is unmetamorphosed. This sequence is related to the Late Cretaceous arc/back-arc magmatic activity of the Sredna Gora zone to the north (Sd, in Fig. 5c), whose age is confirmed by the presence of *Globotruncana* taxa [7].

4. Petrologic and geochemical data

The greenschists display acicular texture and foliated fabrics of alternating quartz–mica–albite with chlorite–actinolite-rich domains. Their mineral assemblages and chemical composition and associated volcanic rocks, indicate that their protoliths were of sedimentary and volcanic origin. The basalts in melange-like unit are massive and variolitic lava flows with preserved primary aphyric to porphyric textures. The major phenocrysts are clinopyroxene ± orthopyroxene, plagioclase and Fe–Ti oxides, as well as olivine, when present, set in a microlitic matrix. The clinopyroxene crystallized earlier than plagioclase, as it is included in

the latter; such a crystallization sequence is common in island arc basalt lavas [3]. The basalts are slightly overprinted by secondary minerals, such as chlorite, quartz and calcite, indicative of low-grade metamorphism. Prehnite–pumpellyite assemblages also occur resulting from ocean floor hydrothermal alteration, which have been reported also in Greece [19].

Selected greenschist and basalt samples were analysed by XRF for major and trace elements, and REE abundances were determined by ICP–MS at the University of Lausanne. They show the following characteristics: (a) low abundance of incompatible elements (e.g. Nb); (b) low Nb/Y and P_2O_5/Zr ratios characteristic of tholeiitic basalts; (c) low total REE concentrations. Using relatively immobile trace elements, the geochemical nature of basalts and greenschist has been defined on several discriminative diagrams. In a Zr/TiO_2 vs. Nb/Y plot [34] (Fig. 4a), samples fall in or near the sub-alkaline basalt field. Major and trace element abundances of lavas classify them as low-K and very low-Ti tholeiitic basalts, with some boninitic affinity on Ni vs. Ti/Cr plot [27]. Most samples plot in the island arc basalt field (Fig. 4b and c) except some of semi-pelitic schists, and all basalts fall below $Zr/Y = 3.0$ ratio line on the Zr–Zr/Y diagram (Fig. 4b), typical for basalts erupted in intra-oceanic island arc setting [24]. The REE patterns (Fig. 4d) display LILE enrichment relative to the HFS elements, indicative of depleted mantle source. Basalt samples LREE depletion and slight HREE enrichment reflect subduction-related component [26]. The negative Nb and Ce anomaly consistently points to an island-arc environment, as shown by discrimination diagrams. Overall, trace element discrimination and REE patterns provide strong constraints for an origin of both rock types in a volcanic (intra-oceanic) island arc tectonic setting. Possible contamination by crustal material before their final emplacement is likely.

5. Discussion and geodynamic implications

Petrologic and geochemical signature of greenschists and basalts strongly suggests a volcanic arc origin, which taken collectively with similar data and ages in Greece, indicates the existence of an intra-oceanic island arc system near the Rhodope continental margin in Middle–Late Jurassic time (Fig. 5a and b). Structural and kinematic data highlight the deformation history of the Mesozoic schists. The NW–NNE-directed shear in greenschist facies demonstrates a ductile-brittle tectonic emplacement. The northeast-directed shear is interpreted as related to detachment faulting, but with opposing sense of shear to that of the basement detachment, whose both surfaces have contributed to strong thinning, in between, of the marble-schist unit. However, northwest-directed shear possibly reflects an earlier thrusting event, which could represent deformation in a subduction–accretion complex. The low-grade rocks have escaped the Cretaceous UHP/HP conditions (Balkan orogenic events) recorded in the immediately underlying basement of the studied area [18], but high-pressure relics are preserved in Chalkidiki [21]. This suggests that they have been transferred to the upper plate in a supracrustal position. This is confirmed, in the Serbo-Macedonian domain, by ophiolites and CRB rocks found on top of the crystalline basement. They seem to have been involved in ENE-directed unroofing of Serbo-Macedonian basement rocks above the lower Rhodopian nappes, with lately reworked contact and omissions by Tertiary extensional tectonics [16]. These rocks remained in an upper plate position during the renewed Late Cretaceous subduction of the remnant Vardar ocean under the Rhodope, followed by the collision with the Pelagonian terrane and the Palaeocene closure of that ocean (Fig. 5c). The SSW-directed kinematics in the basement unit typically reflects the main syn-metamorphic deformation [9], as well as Eocene–Oligocene late-orogenic extension in this part of the eastern Rhodope [17]. We suggest on account of geochemical features and structural data, that the deformation history of Mesozoic schists corresponds to the Early Cretaceous tectonic emplacement related to ophiolite obduction onto the already accreted CRB domain and Rhodopian margin [22]. Later, the schists were strongly affected by Tertiary low-angle normal faulting.

The palaeotectonic reconstructions in the western Tethys [28,29,35] have shown sequential back-arc basin openings along the Eurasian margin from the Late Permian–Triassic to Early–Middle Jurassic time, due to the Palaeotethys closure and Neotethys widening. The Meliata–Maliac Ocean had been separated from the Neotethys, and was affected by intra-oceanic subduction zone during Jurassic times (Fig. 5a). This

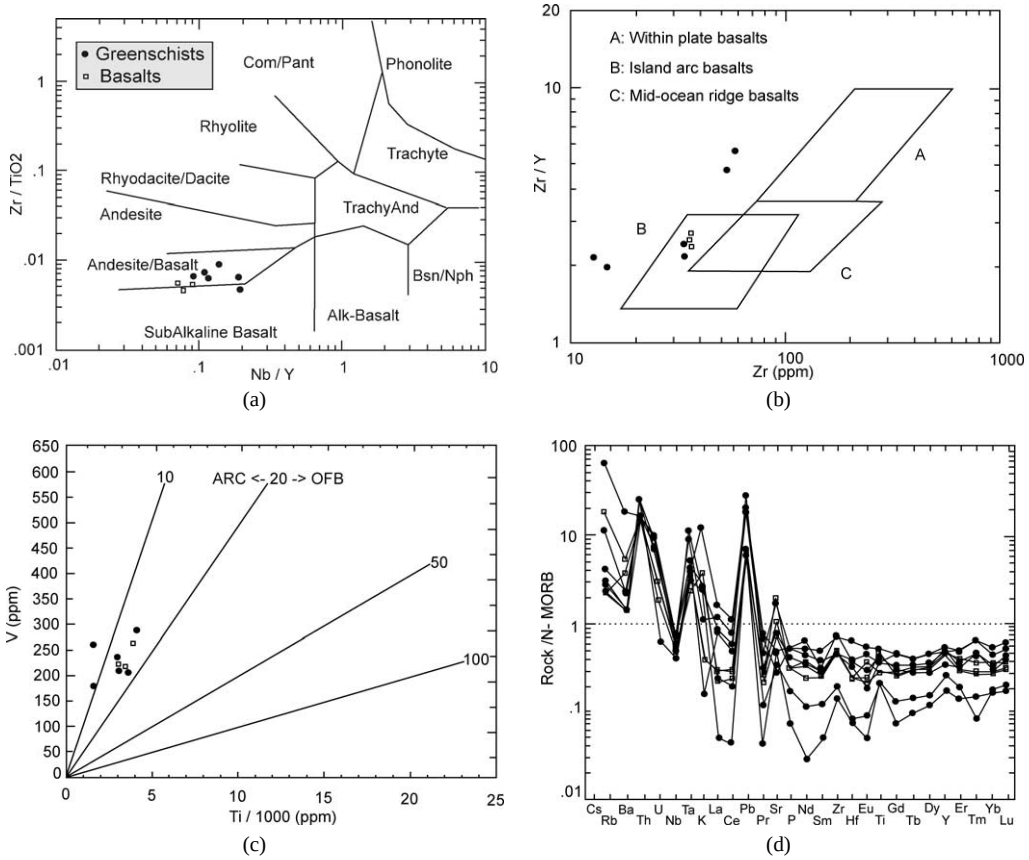

Fig. 4. (**a**) Zr/TiO_2–Nb/Y plot [34]; (**b**) Zr–Zr/Y plot [24]; (**c**) Ti–V plot [27]; (**d**) N-MORB normalized multi-element plot, normalized factors [30].

Fig. 4. (**a**) diagramme Zr/TiO_2–Nb/Y [34] ; (**b**) diagramme Zr–Zr/Y [24] ; (**c**) diagramme Ti–V [27] ; (**d**) diagramme multi-element, normalisé aux facteurs N-MORB [30].

subduction and slab roll-back of Meliata gave birth to a new back arc basin – the Vardar ocean, which by Late Jurassic time had replaced the Meliata–Maliac ocean (Fig. 5b). Our results from the Mesozoic units of eastern Rhodope and western Turkey [2] fit this palaeogeographic framework. We consider that the Meliata–Maliac ocean northern passive margin (Rhodopian lower plate) could be the only source for the olistostromic Upper Permian siliciclastics and carbonates and Middle–Upper Triassic limestone blocks found within the melange-like unit, whereas turbidites and basic lavas originated in an island arc/accretionary complex (upper plate) or possibly from the already accreted CRB domain. The latter corresponds to a segment of the Middle–Late Jurassic intra-oceanic Vardarian island arc system, related to the northwestward slab retreat (roll-back) of the Meliata–Maliac Ocean. The collision of the CRB with the Rhodopian margin followed by the obduction of the intra-oceanic arc (Mandrica–Melia units) resulted in the Early Cretaceous Balkan orogen, which can be followed up to the Carpathians and Eastern Alps [12]. The same Vardarian island arc system collided also with the Pelagonian margin, and provoked a large-scale Late Jurassic–Early Cretaceous ophiolitic obduction in the Hellenides–Dinarides (Fig. 5b). Subduction reversal (northeast-directed subduction of the remnant Vardar) in Late Cretaceous times gave birth to the Srenogorie arc [14] and to the back-arc extension of the Black Sea region (Fig. 5c).

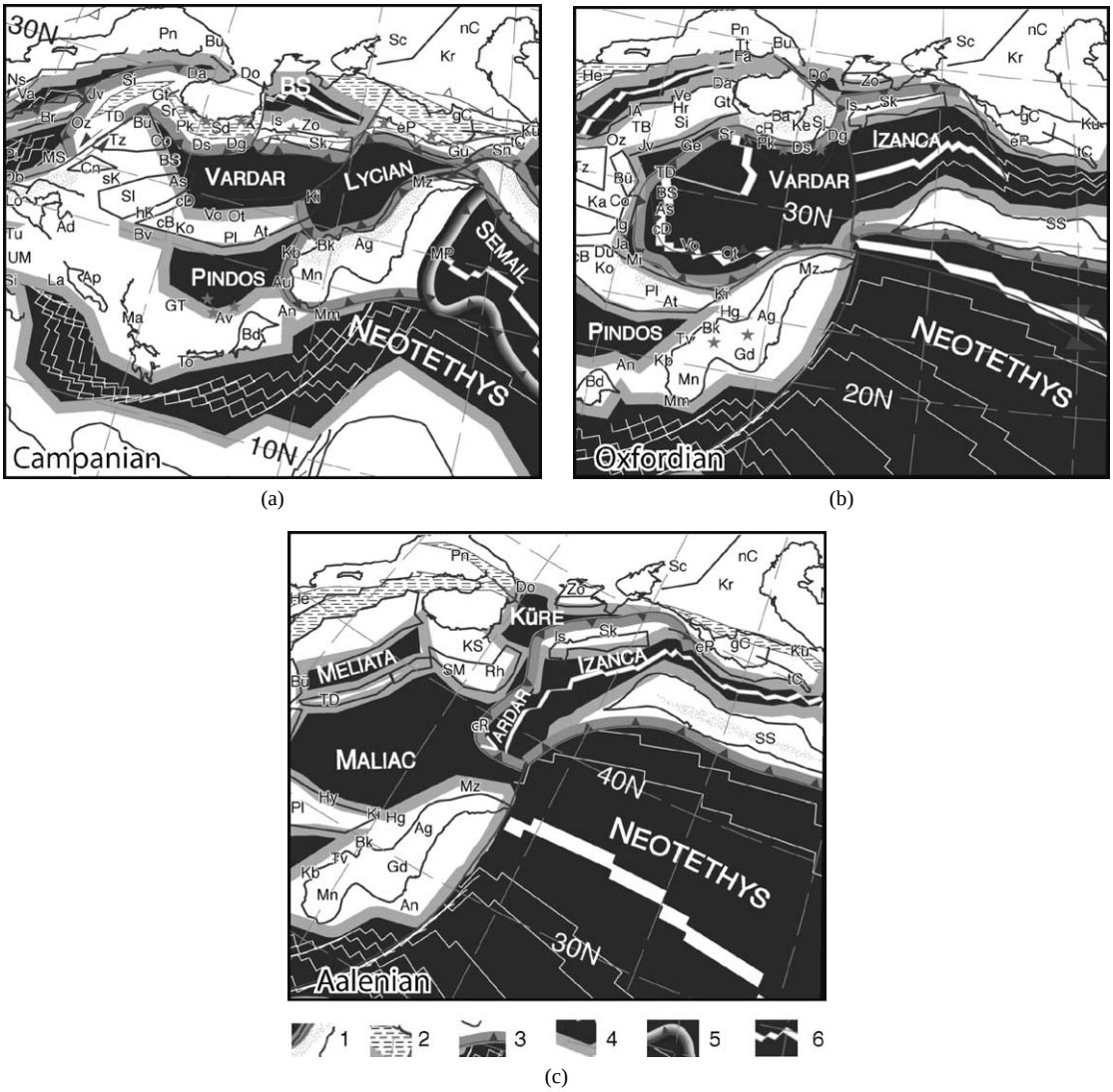

Fig. 5. Palaeotectonic reconstructions after [29]: (**a**) Early Jurassic 180 Ma; (**b**) Late Jurassic 155 Ma, (**c**) Late Cretaceous 84 Ma. **1**, Foreland basin; **2**, rift; **3**, active margin; **4**, passive margin; **5**, intra-oceanic arc; **6**, spreading ridge & ocean. **Ad**, Adria s.str.; **Ag**, Aladag; **An**, Antalya; **Ap**, Apulia s.str.; **As**, Apuseni-south, ophiolites; **At**, Attika; **Au**, Asterousia; **Av**, Arvi; **Ba**, Balkanides, external; **Bd**, Beydaghlari; **Bk**, Bolkardag; **BS**, Bator–Szarvasko ophiolites; **Bu**, Bucovinian; **Bü**, Bükk; **Bv**, Budva; **cB**, central Bosnia; **cD**, central Dinarides ophiolites; **Co**, Codru; **Cn**, Carnic–Julian; **cR**, circum-Rhodope; **Da**, Dacides; **Db**, Dent Blanche; **Dg**, Denizgören ophiolite (IP suture); **Do**, Dobrogea; **Ds**, Drimos ophiolites; **Du**, Durmitor; **eP**, east Pontides; **Fa**, Fatric; **gC**, great Caucasus; **Gd**, Geydag; **Ge**, Gemeric; **GT**, Gavrovo–Tripolitza; **Gt**, Getic; **Gü**, Gümüshane; **He**, Helvetic rim basin; **Hg**, Huglu; **hK**, high karst; **Hr**, Hronicum; **Ig**, Igal trough; **Is**, Istanbul; **Ja**, Jadar; **Jv**, Juvavic; **Ka**, Kalnic; **Kb**, Karaburun; **Ke**, Kotel flysch; **Ki**, Kirshehir; **Ko**, Korab; **KS**, Kotel-Stranja rift; **Ku**, Kura; **iA**, Lower Austroalpine; **La**, Lagonegro; **Lo**, Lombardian; **Ma**, Mani; **Mi**, Mirdita autochton; **Mm**, Mamonia accretionary complex; **Mn**, Menderes; **MP**, Mersin, Pozanti ophiolites; **MS**, Margna-Sella; **Mz**, Munzur dag; **nC**, north Caspian; **Ot**, Othrys–Evia–Argolis ophiolites; **Oz**, Otztal–Silvretta; **Pi**, Piemontais; **Pk**, Paikon intra-oceanic arc; **Pl**, Pelagonian; **Pn**, Pienniny rift; **Rh**, Rhodope; **Sc**, Scythian platform; **Sd**, Srednogorie rift-arc; **Si**, Sicanian; **Sj**, Strandja; **Sk**, Sakarya; **sK**, south-Karawanken fore-arc; **Sl**, Slavonia; **SM**, Serbo-Macedonian; **Sn**, Sevan ophiolites; **Sr**, Severin ophiolites; **SS**, Sanandaj–Sirjan; **TB**, Tirolic-Bavaric; **tC**, Transcaucasus; **TD**, Trans-Danubian; **To**, Talea Ori; **Tt**, Tatric; **Tu**, Tuscan; **Tz**, Tizia; **UM**, Umbria-Marches; **Va**, Valais trough; **Ve**, Veporic; **Vo**, Vourinos (Pindos)–Mirdita ophiolites; **Zo**, Zonguldak.

Fig. 5. Reconstructions paléotectoniques d'après [29]. (**a**) Jurassique inférieur 180 Ma ; (**b**) Jurassique supérieur 155 Ma ; (**c**) Crétacé supérieur 84 Ma. **1**, bassin d'avant-pays ; **2**, rift ; **3**, marge active ; **4**, marge passive ; **5**, arc intra-océanique, **6**, océan et rides médio-océaniques.

These new structural and petrologic data shed a new light on the tectonic setting of the Mesozoic units and their geodynamic context in the frame of the Early Jurassic to Late Cretaceous evolution of the Vardar Ocean. The subduction–accretion history along the limits of the Rhodope metamorphic province has been recently lively debated [1,11,21,22]. The subduction setting of Mesozoic schists situated near the Rhodope margin in pre-Cretaceous time was generally adopted as a possibility [25]. Early Cretaceous cooling of the accretionary wedge by underplating of weakly metamorphosed material may have resulted in emplacement of Mesozoic schists onto the margin and clearly reinforce the maximum allochtonous hypothesis in view of regional correlations and interpretation [11,16,21]. Obviously, the Mesozoic schists were strongly reworked by late extensional and strike-slip tectonics in the entire CRB belt [16,25]. More studies are necessary to unravel the significance of the Circum-Rhodope belt, and test the model of a 'single' Vardar Ocean, but that developed several arc systems.

6. Conclusions

From our field and laboratory studies of the Rhodopian upper nappe system, we can draw the following conclusions. (1) The Mesozoic schists form allochthonous sheets found above the crystalline basement, they present complex internal deformation that could preserve relics of Late Jurassic–Early Cretaceous subduction–accretion tectonic processes, and mainly reflect strong imprint of Tertiary late-orogenic extension. (2) Petrologic and geochemical characteristics of the greenschists and basalts define their island-arc signature, and their protoliths as being derived from depleted mantle source. (3) These results indicate their origin in a Vardarian intra-oceanic island-arc setting during the Middle–Late Jurassic, whose collision with the Rhodope promontory was responsible for the Early Cretaceous north-directed Balkan orogenic system.

Acknowledgements

Post-doctoral research grant to NB from L'AUF is gratefully acknowledged. Critical reviews and valuable suggestions from J.-P. Burg and A. Michard helped to improve the content of the article and were highly appreciated.

References

[1] S.R. Barr, S. Temperley, J. Tarney, Lateral growth of the continental crust through deep level subduction-accretion: a re-evaluation of central Greek Rhodope, Lithos 46 (1999) 69–94.
[2] L. Beccaletto, Geology, correlations, and geodynamic evolution of the Biga peninsula (NW Turkey), PhD thesis, University of Lausanne, 2003, p. 149.
[3] L. Beccaluva, P.D. Girolamo, G. Macciotta, V. Morra, Magma affinities and fractionation trends in ophiolites, Ofioliti 8 (1983) 307–324.
[4] G. Biggazzi, A. Del Moro, F. Innocenti, K. Kyriakopoulos, P. Manetti, P. Papadopoulos, P. Norelliti, A. Magganas, The magmatic intrusive complex of Petrota, west Thrace: age and geodynamic significance, Geol. Rhodopica 1 (1989) 290–297.
[5] I. Boyanov, K. Bodurov, Triassic conodonts in carbonate breccia within the low-grade metamorphic rocks of the East Rhodopes, Geol. Balc. 9 (1979) 97–104.
[6] I. Boyanov, A. Goranov, Late Alpine (Palaeogene) superimposed depressions in parts of Southeast Bulgaria, Geol. Balc. 31 (2001) 3–36.
[7] I. Boyanov, K.M. Ruseva, E. Dimitrova, First find of Upper Cretaceous foraminifers in East Rhodopes, Geol. Balc. 4 (1982) 20.
[8] I. Boyanov, M. Ruseva, V. Toprakcieva, E. Dimitrova, Lithostratigraphy of the Mesozoic rocks from the Eastern Rhodopes, Geol. Balc. 20 (1990) 3–28.
[9] J.-P. Burg, L.-E. Ricou, L. Klain, Z. Ivanov, D. Dimov, Crustal-scale thrust complex in the Rhodope Massif. Evidence from structures and fabrics, in: A.E.M. Nairn, L.-E. Ricou, B. Vrielynck, J. Dercourt (Eds.), The Ocean Basins and Margins: the Tethys Ocean, Vol. 8, Plenum Press, New York, 1995, pp. 125–149.
[10] A. Del Moro, F. Innocenti, C. Kyriakopoulos, P. Manetti, P. Papadopoulos, Tertiary granitoids from Thrace (northern Greece): Sr isotopic and petrochemical data, N. Jb. Miner. Abh. 159 (1988) 113–135.
[11] D.A. Dinter, Late Cenozoic extension of the Alpine collisional orogen, northeasterrn Greece: origin of the north Aegean basin, Geol. Soc. Am. Bull. 110 (1998) 1208–1230.
[12] P. Faulp, M. Wagreich, Late Jurasic to Eocene palaeogeography and geodynamic evolution of the Eastern Alps, Mitt. Österr. Geol. Ges. 92 (1999) 79–94.
[13] J. Ferrière, A. Stais, Nouvelle interprétation de la suture téthysienne vardarienne d'après l'analyse des séries de Péonias (Vardar oriental, Hellénides internes), Bull. Soc. géol. France 166 (4) (1995) 327–339.
[14] G. Georgiev, C. Dabovski, G. Stanisheva-Vasileva, East Srednogorie-Balkan rift zone, in: P.A. Ziegler, W. Cavazza, A.H.F. Robertson, S. Crasquin-Soleau (Eds.), Peri-Tethys Memoir 6: Peri-Tethyian Rift/Wrench Basins and Passive Margins, Mém. Mus. Natl Hist. Nat. Paris 186 (2001) 259–294.

[15] G. Kauffmann, F. Kockel, H. Mollat, Notes on the stratigraphic and paleogeographic position of the Svoula formation in the Innermost Zone of the Hellenides (Northern Greece), Bull. Soc. géol. France 18 (1976) 225–230.
[16] A. Kilias, G. Falalakis, D. Mountrakis, Cretaceous–Tertiary structures and kinematics of the Serbomacedonian metamorphic rocks and their relation to the exhumation of the Hellenic hinterland (Macedonia, Greece), Int. J. Earth Sci. 88 (1999) 513–531.
[17] A. Krohe, E. Mposkos, Multiple generation of extensional detachments in the Rhodope Mountains (northern Greece): evidence of episodic exhumation of high-pressure rocks, in: D. Blundel, F. Neubauer, A. v. Quadt (Eds.), The Timing and Location of Major Ore Deposits in a Evolving Orogen, Geol. Soc. Lond. Spec. Publ. 206 (2003) 151–178.
[18] A. Liati, D. Gebauer, R. Wysoczanski, U–Pb SHRIMP-dating of zircon domains from UHP garnet-rich mafic rocks and late pegmatoids in the Rhodope zone (N. Greece), evidence for Early Cretaceous crystallization and Late Cretaceous metamorphism, Chem. Geol. 184 (2002) 281–299.
[19] A.C. Magganas, Constraints on the petrogenesis of Evros ophiolite extrusives, NE Greece, Lithos 65 (2002) 165–182.
[20] G. Maratos, B. Andronopoulos, Nouvelles données sur l'âge des phyllites du Rhodope, Bull. geol. Soc. Greece 6 (1965) 113–132.
[21] A. Michard, Découverte du faciès schiste bleu dans les nappes du Circum–Rhodope : un élément d'une ceinture HP-LT éohellénique en Grèce septentrionale ?, C. R. Acad. Sci. Paris 318 (1994) 1535–1542.
[22] A. Michard, Supra-ophiolitic formations from the Thessaloniki nappe (Greece), and associated magmatism: an intra-oceanic subduction predates the Vardar obduction, C. R. Acad. Sci. Paris 327 (1998) 493–499.
[23] P. Papadopoulos, N. Arvanitidis, I. Zanas, Some preliminary geological aspects on the Makri unit (Phyllite series), Peri-Rhodope Zone, Geol. Rhodopica 1 (1989) 34–42.
[24] J.A. Pearce, Trace element characteristics of lavas from destructive plate boundaries, in: R.S. Thorpe (Ed.), Orogenic Andesite Related Rocks, Wiley, Chichester, 1982, pp. 525–548.
[25] L.-E. Ricou, J.-P. Burg, I. Godfriaux, Z. Ivanov, The Rhodope and Vardar: the metamorphic and the olistostromic paired belts related to the Cretaceous subduction under Europe, Geodin. Acta 11 (1998) 285–309.
[26] A. Saunders, J. Tarney, Back-arc basins, in: P.A. Floyd (Ed.), Oceanic Basalts, Blackie, Glasgow, 1991, pp. 219–263.
[27] J.W. Shervais, Ti–V plots and the petrogenesis of modern ophiolitic lavas, Earth Planet. Sci. Lett. 57 (1982) 101–118.
[28] G.M. Stampfli, J.D. Borel, A plate tectonic model for the Paleozoic and Mesozoic constrained by dynamic plate boundaries and restored synthetic oceanic isochrons, Earth Planet. Sci. Lett. 196 (2002) 17–33.
[29] G.M. Stampfli, J. Mosar, P. Favre, A. Pillevuit, J.-C. Vannay, Permo-Triassic evolution of the western Tethyan realm: the Neo-Tethys east Mediterranean basin connection, in: P.A. Ziegler, W. Cavazza, A.H.F. Robertson, S. Crasquin-Soleau (Eds.), Peri-Tethys Memoir 6: Peri-Tethyian Rift/Wrench Basins and Passive Margins, Mém. Mus. Natl Hist. Nat. Paris 186 (2001) 51–108.
[30] S.S. Sun, W.F. Mc Donough, Chemical and isotopic systematics of ocean basalts: implications for mantle composition and processes, in: A.D. Saunders, M.J. Norry (Eds.), Magmatism in Ocean Basins, Geol. Soc. Lond. Spec. Publ. 42 (1989) 313–345.
[31] L.B. Tikhomirova, I. Boyanov, I. Zagorchev, Early Jurassic Radiolarians from the Eastern Rhodopes: a revision of the age of Dolno Lukovo Formation, Geol. Balc. 18 (1988) 58.
[32] E. Trifonova, I. Boyanov, Late Permian foraminifers from rock fragments in the Mesozoic phyllitoid formation of the East Rhodopes, Bulgaria, Geol. Balc. 16 (1986) 25–30.
[33] B. Tsikouras, G. Pe-Piper, K. Hatzipanagiotou, A new date for an ophiolite on the northeastern margin of the Vardar Zone, Samothraki, Greece, N. Jb. Miner. Mh. 11 (1990) 521–527.
[34] J.A. Winchester, P.A. Floyd, Geochemical discrimination of different magma series and their differentiation products using immobile elements, Chem. Geol. 20 (1977) 325–343.
[35] P.A. Ziegler, G.M. Stampfli, Late Paleozoic–Early Mesozoic plate boundary reorganisation: collapse of the Variscan orogen and opening of Neotethys, in: R. Cassinis (Ed.), The Continental Permian of the Southern Alps and Sardinia (Italy): Regional Reports and General Correlations, Ann. Mus. Civico Sci. Nat., Brescia 25 (2001) 17–34.